Fitoterapia 127 (2018) 212–219

Contents lists available at ScienceDirect

Fitoterapia

journal homepage: www.elsevier.com/locate/fitote

The influence of natural deep eutectic solvents on bioactive natural products: studying interactions between a hydrogel model and *Schisandra chinensis* metabolites

Yang Liu[a,1], Yu Zhang[b,1], Shao-Nong Chen[a,c,d], J. Brent Friesen[a,c,d,f], Dejan Nikolić[a,c], Mary P. Choules[a,e], James B. McAlpine[a,d,e], David C. Lankin[a,c], Richard A. Gemeinhart[b,g,h,*], Guido F. Pauli[a,c,d,e,f,**]

[a] Department of Medicinal Chemistry and Pharmacognosy, College of Pharmacy, University of Illinois at Chicago, Chicago, IL 60612, USA
[b] Department of Biopharmaceutical Sciences, College of Pharmacy, University of Illinois at Chicago, Chicago, IL 60612, USA
[c] UIC/NIH Center for Botanical Dietary Supplements Research, College of Pharmacy, University of Illinois at Chicago, Chicago, IL 60612, USA
[d] Center for Natural Product Technologies (CENAPT), College of Pharmacy, University of Illinois at Chicago, Chicago, IL 60612, USA
[e] Institute for Tuberculosis Research, College of Pharmacy, University of Illinois at Chicago, Chicago, IL 60612, USA
[f] Physical Sciences Department, Rosary College of Arts and Sciences, Dominican University, River Forest, IL 60305, USA
[g] Departments of Bioengineering and Chemical Engineering, University of Illinois at Chicago, Chicago, IL 60607, USA
[h] Department of Ophthalmology and Visual Sciences, University of Illinois at Chicago, Chicago, IL 60612, USA

ARTICLE INFO

Keywords:
Natural deep eutectic solvent (NADES)
Hydrogel
Drug delivery
Schisandra chinensis
Natural products bioavailability

ABSTRACT

Natural Deep Eutectic Solvent (NADES) species can exhibit unexpected solubilizing power for lipophilic molecules despite their simple composition: hydrophilic organic molecules and water. In the present study, the unique properties of NADES species were applied in combination with a model polymer system: a hydrophilic chitosan/alginate hydrogel. Briefly, NADES species (e.g., mannose-dimethylurea-water, 2:5:5, mole/mole) formed matrices to 1) dissolve lipophilic molecules (e.g., curcumin), 2) load lipophilic molecule(s) into the hydrogel, and 3) spontaneously vacate from the system. NADES species ubiquitously occur in natural sources, and a crude extract is a mixture of the NADES species and bioactive metabolites. Based on these ideas, we hypothesized that the crude extract may also allow the loading of natural bioactive molecules from a natural NADES species into (bio)hydrogel systems. To evaluate this hypothesis *in vitro*, *Schisandra chinensis* fruit extract was chosen as a representative mixture of lipophilic botanical molecules and hydrophilic NADES species. The results showed that the NADES matrix of *S. chinensis* was capable of loading at least three bioactive lignans (i.e., gomisin A, gomisin J, and angeloylgomisin H) into the polymer system. The lipophilic metabolites can subsequently be released from the hydrogel. The outcomes suggest that a unique drug delivery mechanism may exist in nature, thereby potentially improving the bioavailability of lipophilic metabolites through physicochemical interactions with the NADES.

1. Introduction

NAtural Deep Eutectic Solvent (NADES) species were first recognized in 2011 as botanical liquid media [1]. Since then, additional NADES species have attracted attention due to their solubilizing ability for lipophilic molecules, inspiring applications as extraction and dissolution media [2]. The NADES components are usually hydrophilic molecules [1]. Combined with the power to solubilize lipophilic components, NADES species exhibit a solvent duality (lipophilicity and hydrophilicity), suggesting that they may serve a unique function in lipophilic molecule delivery [3].

Water plays an important role as a NADES component because it can regulate the solubilizing ability of NADES species. For example, when increasing the water content of glucose-choline chloride-water (GCWat), the corresponding rutin solubilities decreased significantly [4]. This may be because the water content in NADES affects the entropy of the matrix and, thus, alters its solute-carrying phase shape or size. In addition, water involvement may cause the matrix to

* Correspondence to: R. A. Gemeinhart, Department of Biopharmaceutical Sciences, College of Pharmacy, University of Illinois at Chicago, Chicago, IL 60612, USA.
** Correspondence to: G. F. Pauli, Department of Medicinal Chemistry and Pharmacognosy, College of Pharmacy, University of Illinois at Chicago, Chicago, IL 60612, USA.
E-mail addresses: rag@uic.edu (R.A. Gemeinhart), gfp@uic.edu (G.F. Pauli).
[1] These authors contributed equally to this work.

https://doi.org/10.1016/j.fitote.2018.02.024
Received 6 November 2017; Received in revised form 18 February 2018; Accepted 19 February 2018
Available online 21 February 2018

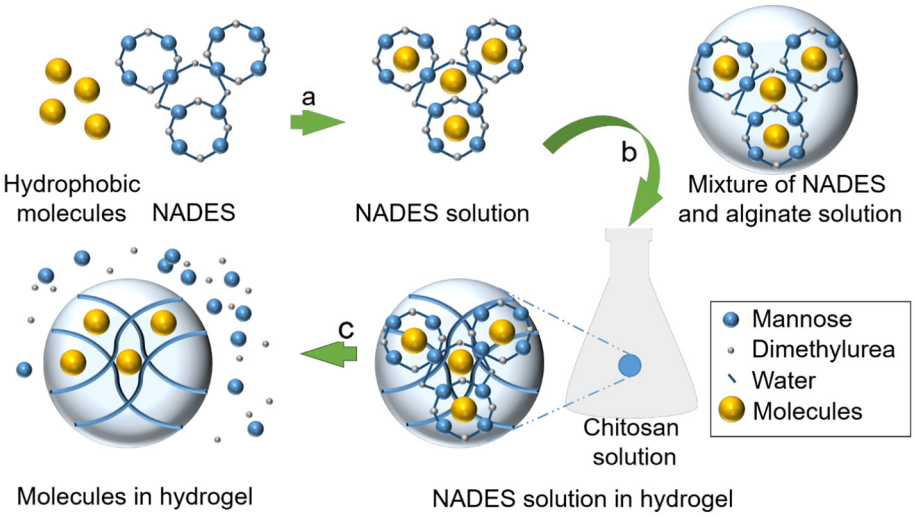

Fig. 1. Model of the loading of hydrophobic molecules into a hydrogel. (a) NADES dissolves the hydrophobic molecules; (b) hydrogel-forming polymers are added to the NADES; (c) due to NADES' dual properties (hydrophilic components capable of dissolving lipophilic molecules), the most of NADES diffuse out of the hydrogel, leaving behind the hydrophobic molecule in the hydrogel.

disassemble and form NADES component solution, associated with the release of dissolved molecules from the matrix (Fig. 1). This dynamic structure of water has been proposed as self-organizing liquid crystals [1].

The collective experience of research on bioactive natural products over the past decades has repeatedly led to the observation that lipophilic components within a crude extract have significantly higher apparent water solubility than the purified individual components. This indicates that a unique mechanism may exist that impacts the practice of traditional medicine and botanical dietary supplements. The present study aims to demonstrate a possible pathway by which NADES species introduce bioactive lipophilic metabolites into biopolymer matrices. Such a natural drug delivery mechanism mediated by NADES species has the potential to support the use of botanical materials and crude extracts beyond the reductionist administration of purified putative bioactive substances.

2. Experimental

2.1. Materials

Choline chloride, chitosan, dimethylurea, D-(+)-fructose, D-(+)-glucose, D-(+)-mannose, maleic acid, sodium alginate, urea, curcuminoid (from *Curcuma longa* (turmeric), powder; CAS: 458-37-7), HPLC grade solvents, and DMSO-d_6 (99.9 atom % D) were purchased from Sigma-Aldrich Inc. (St. Louis, MO, USA). Acetic acid and anhydrous calcium chloride were obtained from Fisher Scientific (Hampton, NH, USA). The fruits of *S. chinensis* were purchased in a local grocery store in the Chinatown neighborhood of Chicago. A voucher specimen (BC 805) has been deposited in the UIC Botanical Center, Chicago, IL.

2.2. Preparation of natural deep eutectic solvent (NADES) and NADES solution

2.2.1. NADES preparation

The ultrasound-centrifuge evaporation method was applied to the preparation of NADES species [3]. The mass of each NADES component was calculated, according to the molar ratios. The solid components were placed into a vial and excess water was added. The mixture was sonicated via an FS140 ultrasonic bath (Fisher Scientific, Loughborough, UK) until dissolved to homogeneity. The solution was then concentrated using a centrifugal vacuum evaporator system (Thermo Scientific, Waltham, MA, USA) for 16 h using an RVT4104 Refrigerated Vapor Trap operating at −105 °C, SC250 Express SpeedVac centrifuge kept at 37 °C, and an OFP 400 Vacuum Pump. Following this evaporation step, the NADES liquid water content was adjusted by adding precise amounts of water. Finally, the sample was placed into an ISOTEMP 110 water bath (Fisher Scientific, Loughborough, UK) at 37 °C until further use.

2.2.2. NADES solutions containing curcumin-enriched material (CEM)

A curcuminoid mixture enriched in its primary phytochemical, curcumin, previously designated as curcumin-enriched material (CEM) was used [5]. CEM (25 mg) was dissolved into 1 mL of NADES. The suspension was homogenized by vortexing for 1 min, placed into an ISOTEMP 110 water bath (Fisher Scientific, Hampton, NH, USA) at 37 °C for 24 h, and then filtered. The resulting saturated solution was stored at 25 °C and placed in the same water bath for 30 min prior to use.

2.3. Preparation of hydrogel beads

A sodium alginate solution (0.2 g/mL) was prepared by dissolving 6 g of sodium alginate in 30 mL of distilled water at 50 °C under constant stirring (Hotplate-Stirrer, Fisher Scientific, Hampton, NH, USA). A chitosan solution (5 mg/mL) was prepared by dissolving 450 mg of chitosan and 5.4 g of anhydrous $CaCl_2$ in 90 mL of distilled water, and 1 mL of acetic acid was added to facilitate chitosan dissolution under constant stirring and heating at 50 °C on the Hotplate-Stirrer until the solid dissolved. The curcumin sample loaded hydrogel beads were prepared with 500 µL of alginate solution and 500 µL of NADES solution combined in a 5 mL test tube: The alginate/NADES mixture was then vortexed (Vortexer 59, Labnet International Inc., Woodbridge, NJ, USA) to obtain a uniform solution, which was transferred into an insulin syringe (0.5 mL, 100 U BD ultra-fine™, EXEL International Medical Products, Redondo Beach, CA, USA). The alginate/NADES solution was added dropwise from the insulin syringe 5 cm above the surface of a 20 mL chitosan/$CaCl_2$ solution in a 50 mL round-bottomed flask under constant stirring. After all beads were formed, the beads were hardened by stirring the solution for another 15 min. A new chitosan solution was used for each group. Beads were collected, and then washed with distilled water 5 times, and 60 mg of wet beads from each group were weighed into different vials and stored at 4 °C before further use.

2.4. Preparation of S. chinensis fruit crude extract

S. chinensis raw fruits were dried at 25 °C, and then ground into small particles using a grinder (KitchenAid - St. Joseph, MI, USA), and stored at 4 °C until use. Raw fruit particles (168 g) were repeatedly extracted with methanol (800 mL, 4×) at 25 °C. The concentrated

crude extract was obtained after evaporation of excess methanol using a rotary evaporator at 37 °C under vacuum. Extraction yield was 62.7% (wt/wt), i.e., 105 g of methanolic extract was obtained.

2.5. Characterization of gomisin J, gomisin A, and angeloylgomisin H

The structural characterization of gomisin J, gomisin A, and angeloylgomisin H was based on NMR (1D ^{1}H, ^{13}C NMR), and high-resolution electrospray ionization-mass spectrometry (HR-ESI-MS). Related spectroscopic physical properties are listed below.

Gomisin J [6], NMR (400 MHz, $CDCl_3$): ^{1}H NMR, δ 6.625 (s, 2H, H-4 and H-11), 5.728 (s, OH, OH-3′), 5.691 (s, OH, OH-12′), 3.930 (s, 3H, H-2′), 3.922 (s, 3H, H-13′), 3.518 (s, 6H, H-1′ and H-14′), 2.549 (dd, 1H, H6a), 2.452 (dd, 1H, H6b), 2.240 (dd, 1H, H9a), 2.017 (dd, 1H, H9b), 1.881 (dddq, 1H, H7), 1.787 (dddq, 1H, H-8), 0.967 (s, 3H, H17), 0.724 (d, 3H, H18); ^{13}C NMR. δ 150.44 (C-1), 137.77 (C-2), 147.62 (C-3), 113.26 (C-4), 135.00 (C-5), 38.96 (C-6), 33.88 (C-7), 41.08 (C-8), 35.33 (C-9), 140.34 (C-10), 110.19 (C-11), 148.82 (C-12), 137.49 (C-13), 150.33 (C-14), 121.53 (C-15), 122.56 (C-16), 21.90 (C-17), 12.67 (C-18), 60.21 (OCH_3, C-1′, C-14′), 61.15 (OCH_3, C-2′, C-13′). ESI-MS: *m/z* 389.1955 $[MH]^+$, (calcd for $C_{22}H_{29}O_6$, 389.1964).

Gomisin A (syn. Schizandrol B) [7], NMR (400 MHz, $CDCl_3$): ^{1}H NMR, δ 6.619 (s, 1H, H-4), 6.478 (s, 1H, H-11), 5.960, 5.956 (d, 2H, H-12′/13′), 3.903 (s, 6H, H-3′ and H-14′), 3.837 (s, 3H, H-2′), 3.517 (s, 3H, H-1′), 2.684 (d, 1H, H6a), 2.578 (dd, 1H, H9a), 2.349 (d, 1H, H6b), 2.327 (dd, 1H, H9b), 1.867 (dq, 1H, H8), 1.252 (s, 3H, H-18), 0.814 (d, 3H, H17); ^{13}C NMR. δ 152.20 (C-1), 140.81 (C-2), 152.39 (C-3), 110.40 (C-4), 132.12 (C-5), 40.59 (C-6), 71.73 (C-7), 42.12 (C-8), 33.78 (C-9), 132.58 (C-10), 106.04 (C-11), 148.00 (C-12), 135.01 (C-13), 141.28 (C-14), 121.93 (C-15), 124.23 (C-16), 15.90 (C-17), 30.20 (C-18), 60.70 (C-1′), 61.12 (C-2′), 56.05 (C-3′), 100.93 (C-12′/13′), 59.75 (C-14′). HR-ESI-MS: *m/z* 439.1740 [M + Na], (calcd for $C_{23}H_{28}O_7Na$, 439.1733).

Angeloylgomisin H [6,8], NMR (400 MHz, $CDCl_3$): ^{1}H NMR, δ 6.691 (s, 1H, H-4), 6.557 (s, 1H, H-11), 5.885 (q, 1H, H-21), 3.908 (s, 3H, H-13′), 3.874 (s, 3H, H-12′), 3.837 (s, 6H, H-2′ and H-3′), 3.543 (s, 3H, H-1′), 2.741 (d, 1H, H6a), 2.702 (dd, 1H, H9a), 2.412 (dd, 1H, H9b), 2.333 (d, 1H, H6b), 1.882 (dq, 1H, H8), 1.760 (d, 3H, H-23), 1.753 (s, 3H, H-22), 1.248 (s, 3H, H18′), 0.846 (d, 3H, H18); ^{13}C NMR. δ 151.93 (C-1), 140.44 (C-2), 152.69 (C-3), 110.20 (C-4), 133.19 (C-5), 40.77 (C-6), 72.12 (C-7), 42.10 (C-8), 34.38 (C-9), 133.97 (C-10), 112.87 (C-11), 151.82 (C-12), 139.79 (C-13), 142.39 (C-14), 122.99 (C-15), 123.33 (C-16), 16.03 (C-17), 30.04 (C-18), 60.93 (C-1′), 61.11 (C-2′), 56.17 (C-3′ and C-12′), 60.77 (C-13′), 165.82 (C-19), 127.75 (C-20), 137.47 (C-21), 15.45 (C-22), 20.47 (C-23). HR-ESI-MS: *m/z* 501.2500 $[MH]^+$, (calcd for $C_{28}H_{37}O_8$, 501.2488).

2.6. Countercurrent separation

An FCPC instrument (185 mL, Kromaton Technologies, Annonay, France) was used for countercurrent separation in this study. A suitable solvent system, hexanes-ethyl acetate-methanol-water (5:5:5:5, v/v) was selected via a TLC-based solvent system methodology [9]. The sample that was released from the hydrogel was diluted with both upper and lower phase (2 mL of each), then loaded into the sample loop (10 mL). The vial was washed three times with lower phase (1 mL/each) and the washings were also loaded into the sample loop. Descending mode (lower phase mobile) was used in all CCS operations. Elution was conducted at 1100 rpm with 8 mL/min flow rate. The resulting fractions were dried by vacuum centrifugal evaporation and subjected to NMR analyses.

2.7. High performance liquid chromatography (HPLC) analyses

Prior to HPLC analysis, the concentrated samples were dissolved in equal volumes of acetonitrile-water (1:1, v/v). Analytical HPLC was performed on a Waters 2695 system using an Agilent ZORBAX SB-C18 column (4.6 × 250 mm, Santa Clara, CA, USA). A 10 μL aliquot from a stock solution (100 μL of curcumin sample saturated NADES solution in 400 μL of methanol) was injected each chromatographic run. A Waters 996 PDA detector was used to monitor the absorbance of the eluent at 390 nm. The mobile phase consisted of methanol/water with a gradient run initiated with 30:70, increasing linearly to 95:5 at 0.8 mL/min, in 15 min, at 25 °C. Preparative HPLC was performed on a Waters 600 controller with a Delta 600 pump and a 717 autosampler, using a YMC-pack ODS-AQ column (10 × 250 mm l.D., Kyoto, Japan). A 100 μL aliquot of the CPC fraction dissolved in methanol was injected. A Waters 2996 PDA detector was used to monitor the absorbance of the eluent at 254 nm. The mobile phase consisted of acetonitrile/water with a gradient run initiated with 60:40, increasing linearly to 95:5 at 1.5 mL/min, in 65 min, at 25 °C. Empower™ software (Waters Corporation, Milford, MA, USA) was used to acquire, process, and analyze the chromatographic data.

2.8. Nuclear magnetic resonance (NMR) analyses

2.8.1. NMR sample preparation

Prior to analysis, each sample was dried under vacuum (< 1 mbar) in a desiccator overnight. Each sample was dissolved in 500 μL DMSO-d_6 delivered with a 1000 μL analytical syringe (Valco Instruments, Baton Rouge, LA, USA). NMR spectra were acquired on a Bruker DPX-360 NMR spectrometer in 5 mm tubes or on a JEOL 400 MHz NMR spectrometer in 3 mm tubes at 25 °C.

2.8.2. NMR acquisition parameters

Acquisition of quantitative ^{1}H NMR (qHNMR) spectra was as follows: 64 scans (NS), 4 dummy scans (DS), 4 s acquisition time (AQ), collecting 64 k of time domain (TD) data, 90 degree excitation pulse, and a relaxation delay (D1) of 60 s. Acquisition of ^{13}C NMR spectra was as follows: 2048 scans (NS), collecting 32 k of time domain (TD) data, and using a relaxation delay (D1) of 2 s. Acquisition of ^{1}H-^{13}C Heteronuclear Single-Quantum Correlation (HSQC) 2D spectra: spectral width (SW) and transmitter frequency offset for channel F2 were the middle and the occupied width of the ^{1}H spectrum, respectively; the analogous center and total width settings were used in the F1 ^{13}C dimension; the F1 T2 value (CNST2) was 150 Hz; 16 scans (NS) were collected per increment. Acquisition of 2D ^{1}H-^{1}H nuclear Overhauser effect spectroscopy (NOESY) NMR spectra was as follows: spectral width (SW) F2 equal to spectral width (SW) F1, transmitter frequency offset for channel F1 was the middle of the ^{1}H spectrum, 16 scans (NS), 8 s relaxation delay (D1), and 400 ms or 600 ms mixing time (D8). Receiver gain (RG) settings were performed in automation (RGA command) for all spectra.

2.8.3. NMR data processing

The spectra were processed using MestReNova v10.0.1 (Mestrelab Research, Santiago de Compostela, Spain) software. For 1D NMR, line resolution was improved by applying a Gaussian-Lorentzian window function (GB 1 and LB −0.3) and four times zero-filling prior to Fourier transformation of the FID. Baseline correction using a 5th order polynomial function and phase correction were performed manually.

3. Results and discussion

3.1. Establishment and evaluation of the hydrogel model

The hydrogel system underlying this study and can be summarized in the following three points (Fig. 1): (a) NADES species are capable of

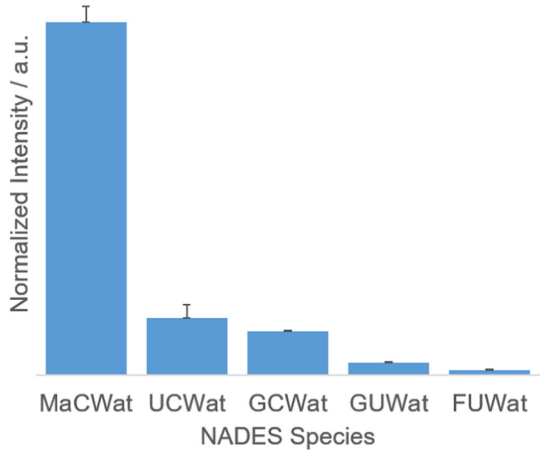

Fig. 2. Solubility of CTE/"curcumin", measured by HPLC determination of curcumin, in different NADES species (n = 3, mean ± SD).

dissolving relatively large amounts of hydrophobic molecules, such as shown for curcumin solubilized in MDWat (Fig. 2). (b) The NADES solution was mixed with an alginate solution, and the mixture was introduced dropwise into the chitosan solution. Once the hydrogel network was formed, the NADES solution is trapped in the micro-environment; (c) Free water can migrate into and out of hydrogel and, thereby, disrupt the NADES matrix. Once the intermolecular interactions among different components in the NADES matrix are disrupted, free NADES components are released from the hydrogel. Because of their hydrophilic nature, NADES components spontaneously diffuse into the aqueous environment by movement down the concentration gradient. Meanwhile, lipophilic molecules are also released from the NADES matrix by passive diffusion. However, because of spontaneous emulsification (aka. The "Ouzo Effect") [10] and precipitation, a part of lipophilic molecules may also be trapped in the hydrogel matrix. Therefore, a controlled released formulation system may be achieved in this model.

3.1.1. Selection of NADES for a given marker compound

To validate this hypothesis, a NADES formulation suitable for the selected marker compounds was developed. With the assistance of Reichardt's dye [11], six NADES species with a broad polarity range were tested, *viz.*: Maleic acid-Choline chloride-Water (MaCWat), Mannose-Dimethyl urea-Water (MDWat), Urea-Choline chloride-Water (UCWat), Glucose-Choline chlorine-Water (GCWat), Glucose-Urea-Water (GUWat), and Fructose-Urea-Water (FUWat). The ratio of the components in each formulation was 2:5:5 (mole/mole).

The focus of this study was to determine, if representative NADES species capable of carrying and loading lipophilic molecules into the hydrogel system. Because of its strong fluorescence and distinctive yellow/orange color, curcumin was selected as a test molecule. Notably, the actual material used in this study was a curcuminoid mixture enriched in its primary phytochemical, curcumin, a material previously designated as curcumin-enriched material (CEM) [5]. The materials represented the residual phytochemical complexity typically encountered in phytopharmaceutical practice. CEM is a refined form of crude curcuminoid-enriched turmeric extract (CTE). While CTE, CEM, and pure/isolated curcumin are often collectively referred to using the same term "curcumin" in the literature, it is important to differentiate these materials clearly [12,13]. It is important to point out that only the most abundant constituent of the test materials, the single compound curcumin, was used as the marker compound in this study. Accordingly, the term CTE/"curcumin" is used throughout the discussion.

The CTE/"curcumin" saturated NADES solutions were examined for curcumin using analytical HPLC. The highest curcumin concentration in the tested NADES was found in MDWat (Fig. 2): The solubility in MDWat was 11 ± 1 mg/mL (n = 3, mean ± SD), which is close to the solubility of CTE in DMSO (12 mg/mL). The selected MDWat composition provided a higher solubility of curcumin than previously reported [14].

To account for the potential water content increase from mixing with the alginate solution, the solubility of CTE/"curcumin" in MDWat at higher water contents, 5% MDWat, (i.e., MDWat: water, 95:5, v/v) was determined (data not shown). The solubility of curcumin in 5% MDWat increased. Thus, when some water was added into the NADES matrix during hydrogel preparation, CTE/"curcumin" did not precipitate. On the other hand, the saturated DMSO solution of CTE/"curcumin" could not be used for the hydrogel preparation because CTE/"curcumin" precipitated once it was mixed with the alginate solution.

3.1.2. Intermolecular interactions in MDWat

To understand the mechanism of MDWat's CTE/"curcumin" solubilizing power, the molecular interaction among the intermolecular components in the MDWat matrix was investigated via the intermolecular nuclear Overhauser effect. To optimize the spectral window, different volume ratios of MDWat to DMSO-d_6, including 1:1, 1:2, 1:5, and 1:10 (v/v) were used to perform 2D nuclear Overhauser effect spectroscopy (NOESY) NMR experiments. The ratio of 1:5 exhibited the desired spectral window, where 1D ^{1}H NMR spectra could be acquired in high resolution and dipole-dipole interactions be determined as well (Fig. 3). The data indicated that the three components of MDWat interact with one another through a complex hydrogen bonding network. Herein, due to the minimization of thermodynamic effects, the dimethylurea (DMU) configuration (Fig. 3) can be assigned to represent the major population. Thus, because of hydrogen bonding between the carbonyl group of DMU and exogenous OH groups (C═O···H−O), the methyl (Me) groups of DMU exhibited interactions with OH groups of mannose. However, the NH groups in DMU exhibited no interaction with mannose (Fig. 3a). In Fig. 3b, dispersive peaks occurred between the signals of water and OH groups of mannose. This is consistent with of hydrogen bonding between water and the OH groups of mannose. As a result, the nOe signals were partially suppressed. It also shows that water may bind predominantly with two OH groups of mannose. Fig. 3c demonstrates that water also hydrogen bonds to the NH groups. All of these observations suggest that the water molecules behave as linkers between the other two NADES components. This also suggests that NADES may be structurally analogous to cyclodextrin, a commonly used excipient in hydrophobic drug formulation [15]. The three MDWat components, i.e., mannose, dimethylurea, and water, may orient themselves forming a complex microstructural hydrophilic outside, as well as a hydrophobic niche inside of MDWat matrix to accommodate hydrophobic compounds, resulting in their superior solubilizing power for hydrophobic molecules. This occurs despite the fact all the components comprising NADES are strongly hydrophilic in nature.

3.1.3. Feasibility of loading in a hydrogel

Alginate is a linear unbranched polysaccharide with (1–4) links, and varying residue amounts of α-L-guluronic, and β-D-mannuronic acids. It is a natural water-soluble polymer extracted from brown algae [16]. Alginate is widely used in pharmaceutical applications as a drug carrier due to good biocompatibility and biodegradability. However, it is challenging to load lipophilic molecules into alginate hydrogels due to the high water content of these drug carriers [17]. However, the hydrogen bonding capabilities of alginates could provide a welcoming environment for NADES, which are composed of hydrophilic components. In order to confirm this hypothesis, a NADES solution and an alginate solution were introduced dropwise into a stirred chitosan/Ca^{2+} solution using an insulin syringe. Subsequently, the test molecule, curcumin, was loaded into the negatively charged alginate hydrogel core, for which Ca^{2+} acts as a crosslinker. The cationic chitosan also interacts with the anionic alginate on the hydrogel to form

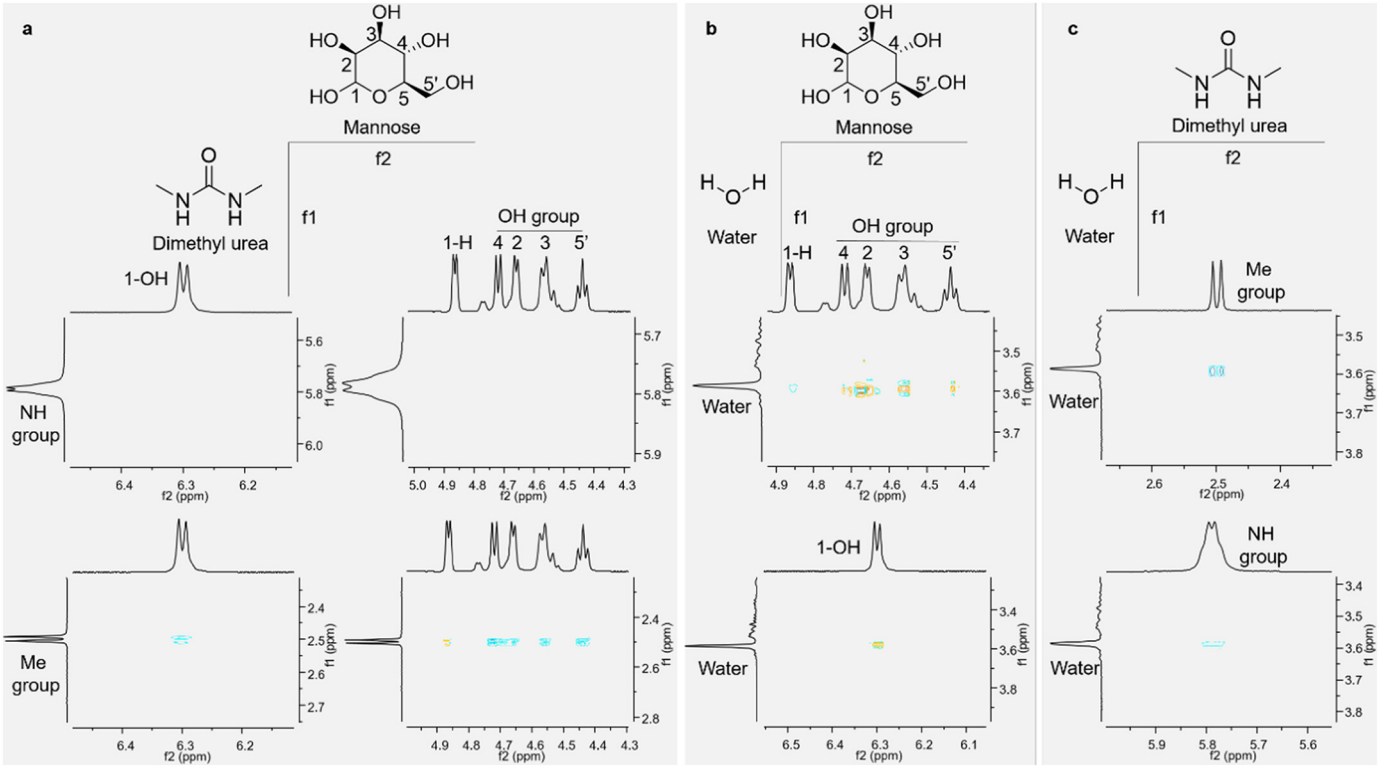

Fig. 3. Nuclear Overhauser effect spectroscopy of MDWat in DMSO-d_6, using an 8 s relaxation delay (D1) and a 0.4 s mixing time (D8). The dipole-dipole interaction between (A) mannose and DMU; (B) mannose and water; (C) DMU and water.

polyelectrolyte complexes, which solidify the hydrogel beads.

3.1.4. Optimization of hydrogel loading concentration

To determine the optimal ratio between the CTE/“curcumin”-MDWat and the alginate solution, hydrogel beads were prepared at 1:3, 1:1, and 3:1 ratios of CTE/“curcumin”-MDWat/alginate (v/v) (Supplementary Information, S1). No curcumin precipitated after vortex mixing, and uniform solutions could be formed at all three ratios. This indicated that the alginate solution did not significantly change or decrease the MDWat solubilizing ability, and the entropy of diluted NADES solution was still in the range of the NADES state. Visual inspection of the hydrogel beads suggests successful encapsulation of curcumin in the hydrogel, as evidenced by the bright orange color. The hydrogel beads successfully packaged the molecules at all of the tested CTE/”curcumin”-MDWat/alginate ratios, (Supplementary Information, S1). However, due to the fact that the alginate quantity determines its inner mesh size [18], at the 1:3 ratio of alginate to MDWat solution, hydrogel beads generally exhibited more irregular sizes and shapes, with porous surfaces. These properties are less favorable for applications where diffusion is the release mechanism. On the other hand, the ratio of alginate to MDWat solution also determined the amount of CTE/”curcumin” loaded. At the 3:1 ratio, the hydrogel beads exhibited a lower quantity of loaded CTE/”curcumin”. Thus, an alginate to CTE/”curcumin”-MDWat solution ratio of 1:1 was selected for the subsequent release assays. Further optimization of the properties for loading using NADES will be examined in future work.

3.1.5. Dynamic change of NADES components

To understand the fate of the NADES components following the hydrogel preparation, a ^{13}C NMR spectrum (Supplementary Information, S2) of the chitosan solution was obtained immediately following removal of the hydrogel beads. Both DMU and mannose were detected in the chitosan solution. The release of mannose and DMU from hydrogel beads was determined by quantitative ^{1}H NMR (qHNMR). As the DMSO solvent signal was superimposed on the methyl group of DMU (Supplementary Information, S3), the solvent could not be used and caffeine was used as internal calibrant instead of the solvent signal. The qHNMR analysis also showed that 94.2% ± 3.9% of the mannose and 91.4% ± 2.8% of the DMU initially present in the exterior phase of the alginate formation media remained after hydrogel bead preparation. This suggests that when the CTE/“curcumin”/NADES/alginate mixture was introduced dropwise into the chitosan solution, mannose and DMU quickly diffused out into the chitosan solution as they are both very soluble in water. Finally, as the prepared beads were washed with fresh water five times, and the mannose and DMU inside the prepared beads should be < 0.01%. It is also plausible that the NADES microstructure may produce micro- or even nanoparticles of lipophilic molecules [3,19]. Thus, the rapid removal of the NADES components from the hydrogel indicated that the curcumin/NADES mixture may experience the spontaneous emulsification during hydrogel preparation [10,20]. Accordingly, the microenvironment inside each alginate bead is capable of switching to non-solvent (water) for the loaded CTE/“curcumin” and the system evolves towards phase separation, leading to the formation of particles. Flocculation of particles and formation of large aggregates are a limitation for nanoprecipitation with spontaneous emulsification [10]. In order to determine if larger crystals or other aggregates were present inside the hydrogel beads, they were stored at 4 °C for 72 h, representing a condition that accelerates nucleation and aggregation. The beads were then sectioned and observed under a microscope. No crystal or large aggregates were observed (Supplementary Information, S4). It is known that the very low solubility of the hydrophobic solute in water and/or homogeneously sized particles opposes growth of larger particles at the expense of smaller ones (Ostwald ripening) [10]. Considering the outcomes, the alginate polymer might also function as a surface coating that prevents molecular agglomeration. This effect has been shown to stabilize the precipitation of β-carotene nanoparticles within a poly (styrene)-β-poly(ethylene oxide) block copolymer [21].

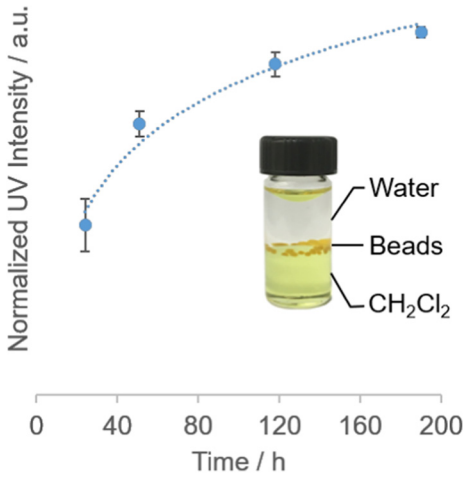

Fig. 4. The release of curcumin from the hydrogel beads into the dichloromethane (syn. CH_2Cl_2) phase of a CH_2Cl_2/water system (1:1, v/v). The release was observed from CTE/"curcumin"-loaded hydrogel beads while suspended in the solvent system (n = 3, mean ± SD).

3.1.6. Investigation of loading efficiency

The ability of the delivery systems to release curcumin was initially assessed using the biphasic solvent system of CH_2Cl_2 and water [22]. Hydrogel beads (60 mg) loaded with CTE/"curcumin" were used, and the release occurred at the two-phase interface (Fig. 4). The yellow color was only present in the CH_2Cl_2 phase. The release occurred over 180 h in this biphasic system (Fig. 4). This indicated that 60 mg of beads may maintain release for at least 180 h in aqueous media, considering the fact that CTE/"curcumin" has a higher solubility in CH_2Cl_2 than in water. The released CTE/"curcumin" was determined via qHNMR using internal calibration with caffeine. Compared to the original curcumin quantity in NADES solution, 13% ± 3% curcumin (n = 3, mean ± SD) was collected in the released sample. The diffusion of similar species of similar size will have similar diffusion coefficients, and thus will be driven to diffuse in a similar manner. Considering the different diffusion capabilities of NADES components and CTE/"curcumin", over 99% NADES components and nearly 87% CTE/"curcumin" constituents were removed in the exterior phase of the alginate formation media remained after hydrogel bead preparation. Collectively, these results boded well for the feasibility of studying the potential interaction between the hydrogel model and lipophilic *S. chinensis* metabolites.

3.2. Interaction between S. chinensis fruit extract and the hydrogels

3.2.1. S. chinensis fruit extract loaded hydrogel

S. chinensis fruit extract exhibited NADES physical nature. Because the extract contained some NADES components (such as citric acid and malic acid, data not shown) and lipophilic ingredients (e.g., lignans), the *S. chinensis* fruit extract presented a similar situation as the modeled MDWat/CTE/"curcumin" matrix. In the preliminary assays, the complexity of the crude extract prevented the formation of a homogeneous mixture with the alginate solution at a ratio of 1:1 (v/v, as Fig. 5A). This may be due to disruption of interactions in the *S. chinensis* fruit extract that suggest either ionic interactions that may be disrupted by the ionic polymers or is further evidence that NADES matrix is being disrupted, and therefore diminishes the solubilty of some components. Therefore, the quantity of alginate solution used in formulation was increased. Several ratios of crude extract to alginate solution were examined: 1:1, 5:1, 10:1, 15:1, and 20:1 (v/v; Fig. 5A). Homogeneous mixtures were obtained with ratios from 5:1 to 20:1 (v/v, Fig. 5B), and the hydrogel beads showed better uniformity at ratios of 10:1, 15:1, and 20:1(v/v). Moreover, as discussed in Section 3.1.4, a high percentage of alginate solution in the homogeneous mixture resulted in a comparatively low

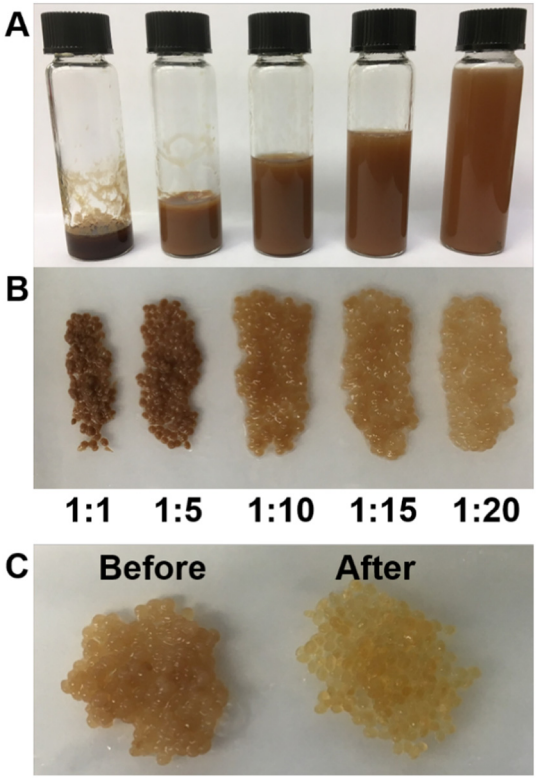

Fig. 5. Hydrogel beads loaded with *Schisandra chinensis* crude extract. The mixture of crude extract and alginate solution (A) was dropped into a chitosan solution to obtain beads (B). The biomass loaded beads (C; labeled as "Before") and after methanol extraction (labeled as "After").

loading capability in the hydrogel beads. Accordingly, the combination of 1 mL of *S. chinensis* fruit extract (1.36 g) and 10 mL of alginate solution was used to investigate the potential interaction between the hydrogel model and *S. chinensis* metabolites. Once the *S. chinensis* metabolites were loaded in the hydrogel beads, our hypothesis is that the proposed pathway may be capable of introducing bioactive lipophilic metabolites into biopolymer matrices via NADES assistance.

The fractionation of *S. chinensis* fruit extract via chromatography on HP-20 resin mostly led to the non-hydrophilic collection of 25% aqueous MeOH and 100% MeOH fractions (Supplementary Information, S5). This indicates that MeOH could be an appropriate extraction solvent for loaded hydrogel beads. Accordingly, 50 mL of MeOH was used as the extraction solvent in a two-day release experiment. The extraction was performed three times, i.e., for a total of 144 h. The combined released metabolites had a 231 mg dry weight. This demonstrates that some non-hydrophilic ingredients have been loaded in the hydrogel beads.

3.2.2. Analysis of released S. chinensis metabolites

Dibenzocyclooctadiene lignans are the major described bioactives of *S. chinensis* fruits [23]. Detection of these lignans in the released metabolites indicated that the NADES species in the crude extract itself may function by the proposed "slow release" mechanism, i.e., that *S. chinensis* fruit extract contains both lipophilic constituents as well as NADES (species). NMR analyses of the released metabolites (Supplementary Information, S6A) demonstrated that fatty acids [24] and some lignans (as evident from the 6–7 ppm region of the spectrum) are among the major components of the *S. chinensis* fruit extract.

For a qualitative investigation of the released metabolites, one step of separation was performed using centrifugal partition chromatography (CPC), representing a liquid-only countercurrent separation method [25]. The solvent system of hexanes-ethyl acetate-methanol-

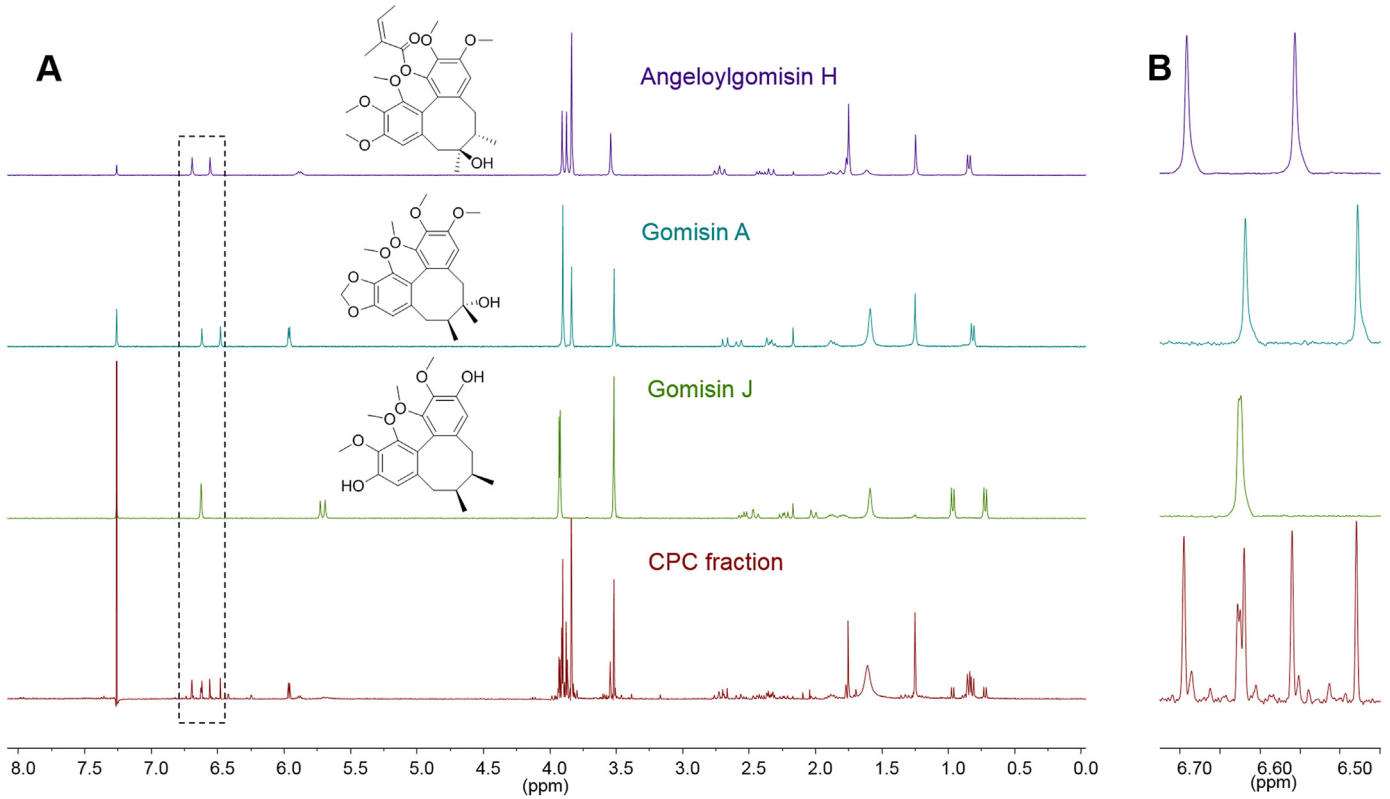

Fig. 6. NMR analysis of the CPC fraction containing the *Schisandra* lignans. (A) Comparison between the CPC fraction and the lignan standards; (B) is an expansion of dashed rectangle in (A).

water (5:5:5:5, v/v) was selected using the GUESS TLC-based solvent system prediction strategy [26,27]. The CPC system gave 0.76 as the stationary phase retention (*Sf*) value. The fractions were concentrated via a centrifugal vacuum evaporator and analyzed by NMR [28]. The eluents were mainly located in two K ranges, i.e., K ≈ 3, and K close to infinity (identified as fatty acids, see Supplementary Information, S6B). NMR analyses of the fractions with K ≈ 3 led to the identification of at least three lignans (Fig. 6A). Based on the characteristic signals of the dibenzocyclooctadiene lignans bearing an eight-membered ring, several methoxy groups, and one aromatic proton in each aromatic ring. Interestingly, both of the aromatic protons give rise to singlets. According to their unique chemical shifts, these signals can be used for the lignan characterization and quantification. To evaluate this hypothesis further, a prep-HPLC fractionation was performed and yielded three lignans: gomisin J (retention time [t_R], 22.0 min), gomisin A (23.5 min), and angeloylgomisin H (26.5 min). Fig. 6B demonstrates that the singlet aromatic protons signals of dibenzocyclooctadiene lignans can be used for their identification.

These results indicate that the NADES existing in crude extracts could potentially contribute to the delivery of bioactive lipophilic metabolites with the assistance of natural biopolymers. Thereafter, this natural “slow release” delivery matrix might assist or enhance the pharmacological function of these lipophilic metabolites of low aqueous solubilities. This proposed natural drug delivery mechanism provides evidence that herbal materials in the form of crude extracts might function as bioavailability enhancer.

4. Conclusions

The present study demonstrates that NADES such as mannose-dimethylurea-water (MDWat, 2:5:5, mole/mole) can behave as “shuttle vectors” which deliver lipophilic molecules dissolved in the NADES into hydrogel beads, and leave some of the lipophilic molecules in the hydrogel beads, then spontaneously diffuse from the polymer carrier during the preparation procedure. The investigated lipophilic therapeutics, CTE/”curcumin” and *Schisandra* lignans, exhibited a significant incorporation into the beads. The bioactive metabolites of *S. chinensis* were successfully loaded into the hydrogel polymer using the NADES matrix in *S. chinensis* fruit extract, and behaved similarly to the test molecules. This study validated the hydrogel model to be equivalent to a biopolymer, capable of absorbing natural metabolites and allowing for their controlled release. Specifically, bioactive lignans (gomisin J, schisandrol B, and angeloylgomisin H) were characterized in the released aliquots. This supports the broader hypothesis that a NADES species (as natural solvents) related mechanism may improve the absorption of lipophilic molecules in traditional botanical medicines and dietary supplements. The established approach may contribute to hepato-protective, anti-inflammatory, and anti-cancer applications [29–35] in the future.

The hydrogels, composed of lipophilic metabolites loaded into chitosan-alginate beads, eliminates the use of organic solvents or surfactants to solubilize lipophilic components. It is composed of all-natural and biodegradable components and has potential for delivery formulation applications. The formulation offers the advantage of controlled release directly at the site of action and prolonged bioactive administration. Because it is still a challenge to load lipophilic drugs into an aqueous hydrogel, the amphiphilicity of NADES species could be a promising solution to overcome this hurdle. As an alternative solvent, the potential NADES effect on a whole organism (e.g., a bacterium) or a substructure of the organism (e.g., a cell) is still a major concern [36], which may limit its applications. This study presents NADES as a delivery “shuttle vector”, which would not stay in the formulation. This avoids the potential impact, and also eliminates the solvent removal step that is needed when using organic solvents or chemical reactions in the preparation of delivery carriers. NADES components of crude extracts (or even raw materials) may help deliver

lipophilic bioactives, and hydrogels may have other uses for synthetic drugs or to enhance delivery of natural bioactives.

Finally, it should be noted that NADES species can have good solubilizing ability for both polar and/or non-polar metabolites. NADES can involve both hydrophilic and lipophilic components. Hydrophilic components with highly electronegative groups can form hydrogen bonding via special dipole-dipole interactions, explaining the polar character of hydrophilic NADES species with polar ingredients [37]. Conversely, due to differences in their capability of hydrogen bonding through electrostatic forces, lipophilic compounds remain relatively passive participants in the hydrophilicity/lipophilicity balance phenomenon. Some NADES species, such as menthol- [38] or fatty acid-based [39] NADES, involve components with electronegative groups and, thus, mainly induce electrostatic interactions between component molecules. These NADES species are often miscible with nonpolar ingredients, a behavior that appears to be counterintuitive at first. Examples for these (perceived) exceptions are eutectic mixtures such as citric acid-menthol [40], which contains both a hydrophilic and a lipophilic component to create a hydrophobic NADES species. The actual hydrophilicity/lipophilicity balance of such eutectic mixtures has to be measured individually. At the same time, hydrophilic, aqueous NADES species can still exhibit an unexpected solubilizing ability for lipophilic natural products [38].

Conflict of interest

The authors declare no conflicts of interest.

Acknowledgements

This work was supported by grants P50 AT000155 and U41 AT008706 from ODS and NCCIH of the National Institutes of Health. This investigation was conducted, in part, in a facility constructed with support from the National Institutes of Health National Center for Research Resources (C06 RR15482). Yang Liu is grateful for a USP Global Fellowship from the U.S. Pharmacopeial Convention. Mary Choules acknowledges funding through grant T32 AT007533 from NCCIH/NIH. Furthermore, support from the NMR team of the CSB at UIC (Chicago, IL), in particular by Dr. Ben Ramirez, is gratefully acknowledged.

Appendix A. Supplementary data

Supplementary data to this article can be found online at https://doi.org/10.1016/j.fitote.2018.02.024.

Furthermore, the original NMR data (FIDs) are made freely available at http://dx.doi.org/10.7910/DVN/JDVALF (Harvard Dataverse).

References

[1] Y.H. Choi, J. van Spronsen, Y. Dai, M. Verberne, F. Hollmann, I.W. Arends, et al., Are natural deep eutectic solvents the missing link in understanding cellular metabolism and physiology? Plant Physiol. 156 (2011) 1701–1705.
[2] Y. Dai, G.-J. Witkamp, R. Verpoorte, Y.H. Choi, Natural deep eutectic solvents as a new extraction media for phenolic metabolites in *Carthamus tinctorius* L, Anal. Chem. 85 (2013) 6272–6278.
[3] Y. Liu, J. Garzon, J.B. Friesen, Y. Zhang, J.B. McAlpine, D.C. Lankin, et al., Countercurrent assisted quantitative recovery of metabolites from plant-associated natural deep eutectic solvents, Fitoterapia 112 (2016) 30–37.
[4] Y. Dai, J. van Spronsen, G.-J. Witkamp, R. Verpoorte, Y.H. Choi, Natural deep eutectic solvents as new potential media for green technology, Anal. Chim. Acta 766 (2013) 61–68.
[5] A. Jaja-Chimedza, B.L. Graf, C. Simmler, Y. Kim, P. Kuhn, G.F. Pauli, et al., Biochemical characterization and anti-inflammatory properties of an isothiocyanate-enriched moringa (*Moringa oleifera*) seed extract, PLoS One 12 (2017) e0182658.
[6] R.B. An, S.H. Oh, G.S. Jeong, Y.C. Kim, Gomisin J With protective effect against t-BHP-induced oxidative damage in HT22 cells from *Schizandra chinensis*, Nat. Prod. Sci. 12 (2012) 134–137.
[7] L. Zhu, B. Li, X. Liu, G. Huang, X. Meng, Purification of six lignans from the stems of *Schizandra chinensis* by using high-speed counter-current chromatography combined with preparative high-performance liquid chromatography, Food Chem. 186 (2015) 146–152.
[8] Y. Ikeya, H. Taguchi, I. Yosioka, H. Kobayashi, The constituents of *Schizandra chinensis* BAILL. III. The structures of four new lignans, gomisin H and its derivatives, angeloyl-, tigloyl- and benzoyl-gomisin H, Chem. Pharm. Bull. 27 (1979) 1576–1582.
[9] Y. Liu, J.B. Friesen, E.M. Grzelak, Q. Fan, T. Tang, K. Durić, et al., Sweet spot matching: A thin-layer chromatography-based countercurrent solvent system selection strategy, J. Chromatogr. A 1504 (2017) 46–54.
[10] E. Lepeltier, C. Bourgaux, P. Couvreur, Nanoprecipitation and the "Ouzo effect": Application to drug delivery devices, Adv. Drug Deliv. Rev. 71 (2014) 86–97.
[11] C. Reichardt, Solvatochromic dyes as solvent polarity indicators, Chem. Rev. 94 (1994) 2319–2358.
[12] K.M. Nelson, J.L. Dahlin, J. Bisson, J. Graham, G.F. Pauli, M.A. Walters, The essential medicinal chemistry of curcumin, J. Med. Chem. 60 (2017) 1620–1637.
[13] K.M. Nelson, J.L. Dahlin, J. Bisson, J. Graham, G.F. Pauli, M.A. Walters, Curcumin may (not) defy science, ACS Med. Chem. Lett. 8 (2017) 467–470.
[14] K.O. Wikene, E. Bruzell, H.H. Tonnesen, Characterization and antimicrobial phototoxicity of curcumin dissolved in natural deep eutectic solvents, Eur. J. Pharm. Sci. 80 (2015) 26–32.
[15] G. Tiwari, R. Tiwari, A.K. Rai, Cyclodextrins in delivery systems: applications, J. Pharm. Bioallied. Sci. 2 (2010) 72–79.
[16] R.R. Torelli-Souza, L.A. Cavalcante Bastos, H.G.L. Nunes, C.A. Camara, R.V.S. Amorim, Sustained release of an antitumoral drug from alginate-chitosan hydrogel beads and its potential use as colonic drug delivery, J. Appl. Polym. Sci. 126 (2012) E409–E418.
[17] T.R. Hoare, D.S. Kohane, Hydrogels in drug delivery: progress and challenges, Polymer 49 (2008) 1993–2007.
[18] B.M. Gillette, J.A. Jensen, M. Wang, J. Tchao, S.K. Sia, Dynamic hydrogels: switching of 3D microenvironments using two-component naturally derived extracellular matrices, Adv. Mater. 22 (2010) 686–691.
[19] O.S. Hammond, D.T. Bowron, K.J. Edler, The effect of water upon deep eutectic solvent nanostructure: An unusual transition from ionic mixture to aqueous solution, Angew. Chem. Int. Ed. 54 (2017) 9782–9785.
[20] S.A. Vitale, J.L. Katz, Liquid droplet dispersions formed by homogeneous liquid–liquid nucleation: "The Ouzo effect", Langmuir 19 (2003) 4105–4110.
[21] Y. Liu, K. Kathan, W. Saad, R.K. Prud'homme, Ostwald ripening of beta-carotene nanoparticles, Phys. Rev. Lett. 98 (2007) 036102.
[22] C.K. Kim, P. Ghosh, C. Pagliuca, Z.J. Zhu, S. Menichetti, V.M. Rotello, Entrapment of hydrophobic drugs in nanoparticle monolayers with efficient release into cancer cells, J. Am. Chem. Soc. 131 (2009) 1360–1361.
[23] Y. Lu, D.F. Chen, Analysis of *Schizandra chinensis* and *Schisandra sphenanthera*, J. Chromatogr. A 1216 (2009) 1980–1990.
[24] J. San José, M.A. Sanz-Tejedor, Y. Arroyo, Effect of fatty acid composition in vegetable oils on combustion processes in an emulsion burner, Fuel Process. Technol. 130 (2015) 20–30.
[25] S. Ignatova, N. Sumner, N. Colclough, I. Sutherland, Gradient elution in counter-current chromatography: a new layout for an old path, J. Chromatogr. A 1218 (2011) 6053–6060.
[26] Y. Liu, J.B. Friesen, J.B. McAlpine, G.F. Pauli, Solvent system selection strategies in countercurrent separation, Planta Med. 81 (2015) 1582–1591.
[27] Y. Liu, J.B. Friesen, L.L. Klein, J.B. McAlpine, D.C. Lankin, G.F. Pauli, et al., The Generally Useful Estimate of Solvent Systems (GUESS) method enables the rapid purification of methylpyridoxine regioisomers by countercurrent chromatography, J. Chromatogr. A 1426 (2015) 248–251.
[28] Y. Liu, S.N. Chen, J.B. McAlpine, L.L. Klein, J.B. Friesen, D.C. Lankin, et al., Quantification of a botanical negative marker without an identical standard: ginkgotoxin in Ginkgo biloba, J. Nat. Prod. 77 (2014) 611–617.
[29] M. Kim, S.J. Lim, H.J. Lee, S.Y. Kim, C.W. Nho, Gomisin J inhibits oleic acid-induced hepatic lipogenesis by activation of the AMPK-dependent pathway and inhibition of the hepatokine fetuin-A in HepG2 cells, J. Agric. Food Chem. 63 (2015) 9729–9739.
[30] Y. Jiang, X. Fan, Y. Wang, H. Tan, P. Chen, H. Zeng, et al., Hepato-protective effects of six schisandra lignans on acetaminophen-induced liver injury are partially associated with the inhibition of CYP-mediated bioactivation, Chem. Biol. Interact. 231 (2015) 83–89.
[31] K. Kang, K.-M. Lee, J.-H. Yoo, H.J. Lee, C.Y. Kim, C.W. Nho, Dibenzocyclooctadiene lignans, gomisins J and N inhibit the Wnt/β-catenin signaling pathway in HCT116 cells, Biochem. Biophys. Res. Commun. 428 (2012) 285–291.
[32] X. Wang, D. Hu, L. Zhang, G. Lian, S. Zhao, C. Wang, et al., Gomisin A inhibits lipopolysaccharide-induced inflammatory responses in N9 microglia via blocking the NF-κB/MAPKs pathway, Food Chem. Toxicol. 63 (2014) 119–127.
[33] E.Y. Ryu, S.Y. Park, S.G. Kim, D.J. Park, J.S. Kang, Y.H. Kim, et al., Anti-inflammatory effect of heme oxygenase-1 toward *Porphyromonas gingivalis* lipopolysaccharide in macrophages exposed to gomisins A, G, and J, J. Med. Food 14 (2011) 1519–1526.
[34] S.B. Lee, C.Y. Kim, H.J. Lee, J.H. Yun, C.W. Nho, Induction of the phase II detoxification enzyme NQO1 in hepatocarcinoma cells by lignans from the fruit of *Schisandra chinensis* through nuclear accumulation of Nrf2, Planta Med. 75 (2009) 1314–1318.
[35] M. Na, T.M. Hung, W.K. Oh, B.S. Min, S.H. Lee, K. Bae, Fatty acid synthase inhibitory activity of dibenzocyclooctadiene lignans isolated from *Schisandra chinensis*, Phytother. Res. 24 (2010) S225–228.
[36] M. Hayyan, M.A. Hashim, A. Hayyan, M.A. Al-Saadi, I.M. AlNashef, M.E. Mirghani, et al., Are deep eutectic solvents benign or toxic? Chemosphere 90 (2013) 2193–2195.
[37] A.P. Abbott, D. Boothby, G. Capper, D.L. Davies, R.K. Rasheed, Deep eutectic solvents formed between choline chloride and carboxylic acids: Versatile alternatives to ionic liquids, J. Am. Chem. Soc. 126 (2004) 9142–9147.
[38] S. Tuntarawongsa, T. Phaechamud, Menthol, borneol, camphor and WS-3 eutectic mixture, Adv. Mater. Res. 506 (2012) 355–358.
[39] D.J.G.P. van Osch, L.F. Zubeir, A. van den Bruinhorst, M.A.A. Rocha, M.C. Kroon, Hydrophobic deep eutectic solvents as water-immiscible extractants, Green Chem. 17 (2015) 4518–4521.
[40] B.D. Ribeiro, C. Florindo, L.C. Iff, M.A.Z. Coelho, I.M. Marrucho, Menthol-based eutectic mixtures: Hydrophobic low viscosity solvents, ACS Sustain. Chem. Eng. 3 (2015) 2469–2477.